



What governs the spread in shortwave forcings in the transient IPCC AR4 models?

T. Storelvmo,¹ U. Lohmann,¹ and R. Bennartz²

Received 19 September 2008; revised 16 November 2008; accepted 2 December 2008; published 13 January 2009.

[1] The coupled global atmospheric-ocean models used for transient simulations in the IPCC AR4 report differences in the present-day shortwave forcing of more than 2 W/m^2 . We show here that about 1.3 W/m^2 of this spread could be explained by the different methods used to calculate cloud droplet number concentration (CDNC) from aerosol mass concentrations. Although we cannot rule out that other forcing agents could yield comparable uncertainties, this strongly points to the aerosol indirect effect as the main contributor to the wide spread in the shortwave forcing reported in IPCC AR4. **Citation:** Storelvmo, T., U. Lohmann, and R. Bennartz (2009), What governs the spread in shortwave forcings in the transient IPCC AR4 models?, *Geophys. Res. Lett.*, **36**, L01806, doi:10.1029/2008GL036069.

1. Introduction

[2] More than three decades ago, *Twomey* [1974] stated the first hypothesis on how anthropogenic aerosols may influence climate through their impact on clouds. According to this hypothesis, often termed the first aerosol indirect effect, an increase in atmospheric pollution will lead to an increase in cloud albedo, all else being equal.

[3] Several decades and hundreds of publications later, aerosol indirect effects on climate are still a puzzle to the scientific community [*Baker and Peter*, 2008], adding uncertainty to future climate projections. While the number of hypotheses on how aerosols may affect clouds, and thereby climate, have increased over this time period, the first aerosol indirect effect (AIE) is the only effect which can be calculated as a pure forcing directly comparable to other natural and anthropogenic forcing agents. In the Intergovernmental Panel on Climate Change (IPCC) fourth assessment report (AR4), the first aerosol indirect effect (AIE) was singled out as the most uncertain contributor to the net anthropogenic forcing of climate [*Forster et al.*, 2007]. Despite the fact that this effect, also named the cloud albedo effect, has been studied extensively in recent decades, the level of understanding of this effect was in IPCC AR4 still characterized as low, radiative forcing estimates varying between -0.22 and -1.85 W/m^2 . Hence, the highest estimates predict the AIE forcing to be comparable to that of greenhouse gases, but of opposite sign. Nevertheless, out of the coupled model simulations presented in IPCC AR4 predicting climate change over the next century, only 9 out of 23 included aerosol indirect effects [*Meehl et al.*, 2007].

[4] Prediction of aerosol indirect effects in numerical models requires a method for calculations of cloud droplet number concentration (CDNC) in the model based on aerosol mass or number concentration. In this paper, we investigate different methods applied to predict CDNC in the IPCC AR4 transient ocean-atmosphere simulations that included the AIE, 4 methods in total. We carry out this CDNC scheme intercomparison in the Integrated Forecasting System (IFS) modelling framework, developed at the European Centre for Medium-Range Weather Forecast (ECMWF). The purpose is to provide an estimate of the spread in anthropogenic forcings caused by the prediction of CDNC alone, by performing a series of model experiments varying the CDNC scheme while all other aspects of the modelling framework are kept unchanged. The uncertainty range for the shortwave radiative forcing (SWRF) of the coupled model simulations in IPCC AR4 [*Meehl et al.*, 2007] spans from -1.6 W/m^2 to $+0.6 \text{ W/m}^2$ for the year 2000. It is suggested that a major contributor to this wide range of SWRFs is the variety of parameterization of the aerosol indirect effect among the models.

2. Model Description and Setup

2.1. Integrated Forecasting System

[5] The global atmospheric modeling tool in this study is the Integrated Forecasting System (IFS), which is the operational forecast model from ECMWF. An extended version of the IFS is also the atmospheric component of an Earth system model currently under development, namely the EC-Earth model (<http://eearth.knmi.nl/>).

[6] All simulations were carried out using a Semi-Lagrangian dynamical core at T95 spectral truncation, 40 levels in the vertical and a dynamical timestep of one hour. The physical schemes in the model most relevant for this study are the warm cloud microphysics scheme and the radiation scheme. The treatment of warm stratiform cloud microphysics follows *Tiedke* [1993]. Cloud condensate and cloud cover are prognostic variables, while precipitation release is diagnosed. Warm-phase clouds form in a model grid box when the relative humidity exceeds a critical height-dependent threshold, and dissipate as a result of evaporation and/or precipitation processes. The cloud droplet effective radius (r_e) is calculated based on cloud droplet number concentration and liquid water content, following the formulation of *Martin et al.* [1994]:

$$r_e = \left(\frac{3LWC}{4\pi\rho_w kN_l} \right)^{1/3} \quad (1)$$

where LWC is the liquid water content, ρ_w is the density of water, N_l is the cloud droplet number concentration and k is

¹Institute for Atmospheric and Climate Sciences, ETH-Zurich, Zurich, Switzerland.

²Department of Atmospheric and Oceanic Sciences, University of Wisconsin-Madison, Madison, Wisconsin, USA.

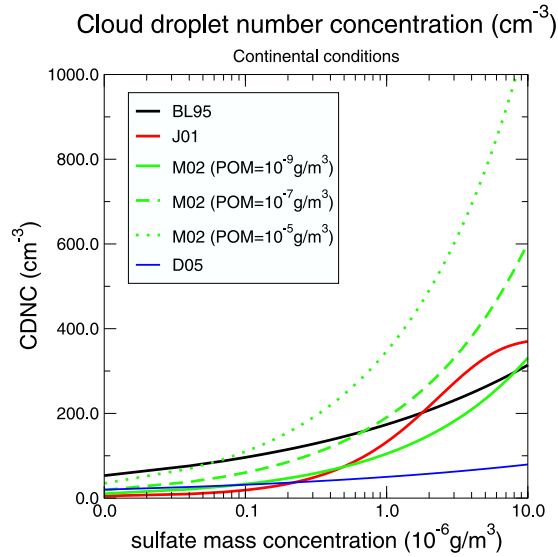


Figure 1. CDNC as a function of sulfate mass concentrations based on equations from BL95, J01, M02 and D05, all for continental conditions. In the M02 case, CDNC is given for 3 different particulate organic matter (POM) concentrations.

a constant (k equals 0.67 over continents, and 0.80 in maritime air masses). Shortwave radiative properties of liquid clouds as a function of cloud droplet effective radius are calculated following *Fouquart* [1987].

2.2. Description of the Aerosol Treatment

[7] As the focus of this study is to assess the forcing uncertainty introduced by applying various CDNC schemes, we prescribed the monthly average aerosol mass concentrations. The aerosol fields are the same as used by *Chen and Penner* [2005] and *Penner et al.* [2006], and include anthropogenic and natural sulfate, black carbon, anthropogenic and natural organic matter, and mineral dust and seasalt aerosols divided into two size categories.

2.3. Description of the Cloud Droplet Schemes

[8] Below follows a short presentation of the 4 methods applied to calculate cloud droplet number concentration (N_l) in this sensitivity study. In all cases N_l is given in cm^{-3} .

2.3.1. Boucher and Lohmann [1995]

[9] The representations of N_l as a function of sulfate mass presented by *Boucher and Lohmann* [1995] (hereinafter referred to as BL95) have been used extensively in model studies of the aerosol indirect effects over the last decade. The empirical relationships in this paper are based on measurements from aircraft campaign carried out over North-America and the North and North-East Atlantic over different seasons and conditions. Based on these measurements, the following two relationships were obtained, for continental and maritime conditions, respectively:

$$N_l = 10^{2.24+0.257 \log(M_{SO_4})} \quad (2)$$

$$N_l = 10^{2.06+0.48 \log(M_{SO_4})} \quad (3)$$

where M_{SO_4} is the sulfate mass concentration in $\mu\text{g}/\text{m}^3$.

2.3.2. Jones et al. [2001]

[10] The CDNC parameterization presented by *Jones et al.* [2001] (hereinafter referred to as J01) was originally presented by *Jones et al.* [1994], but was extended by J01 by taking not only sulfate but also seasalt aerosol concentrations into account. Based on simultaneous aircraft measurements of N_l and number concentrations of sulfate and sea salt aerosols (N_a) from four regions (Pacific ocean, Summer 1987; South Atlantic, Winter 1991; British Isles, Winter 1990 and 1992; Azores, Summer 1992), the following relationship was presented:

$$N_l = \max \left\{ 3.75 \cdot 10^2 \left(1 - e^{-2.5 \cdot 10^{-9} N_a} \right), N_{\min} \right\} \quad (4)$$

[11] Here, N_a represents all sulfate and sea salt aerosols (m^{-3}), and $N_{\min} = 5 \text{cm}^{-3}$. It is assumed that seasalt and sulfate are externally mixed. The number of sulfate aerosols are predicted from the mass concentration of aerosol sulphur (m), following

$$N_{a,SO_4} = 5.125 \cdot 10^{17} m \quad (5)$$

where m is given in kgm^{-3} . The number of seasalt aerosols is calculated as a function of windspeed following the parameterizations of *O'Dowd et al.* [1997, 1999].

2.3.3. Menon et al. [2002]

[12] The relationships between N_l and aerosol mass concentrations presented by *Menon et al.* [2002] (hereinafter referred to as M02) were based on partly the same field campaigns as those presented by BL95. However, they extended the BL95 approach by taking into account not only sulfate mass, but also seasalt and organic mass concentrations, obtaining the following relationships (for continental and maritime conditions, respectively):

$$N_l = 10^{2.41 + \log(M_{SO_4}^{0.50} M_{OM}^{0.13})} \quad (6)$$

$$N_l = 10^{2.41 + \log(M_{SO_4}^{0.50} M_{OM}^{0.13} M_{SS}^{0.05})} \quad (7)$$

where M_{SO_4} , M_{OM} and M_{SS} are the mass concentrations in $\mu\text{g}/\text{m}^3$, of sulfate, organic matter and seasalt respectively.

2.3.4. Dufresne et al. [2005]

[13] *Dufresne et al.* [2005] (hereinafter referred to as D05) presented modified versions of the relationships presented by BL95. By fitting (2) and (3) to satellite data from the POLDER instruments, they obtained the following relationship:

$$N_l = 10^{1.7+0.2 \log(M_{SO_4})} \quad (8)$$

[14] CDNCs as a function of sulfate mass concentration based on Equations 1, 4, 6 and 8 are shown in Figure 1, illustrating the wide range of CDNCs arising from the four methods outlined above. For a given sulfate mass concentration, CDNC estimates span approximately one order of magnitude, especially when moderate amounts of organic matter are allowed to contribute to droplet formation by M02.

2.4. Model Setup

[15] For each CDNC scheme we carried out a pair of simulations; one with preindustrial (PI) aerosol concentra-

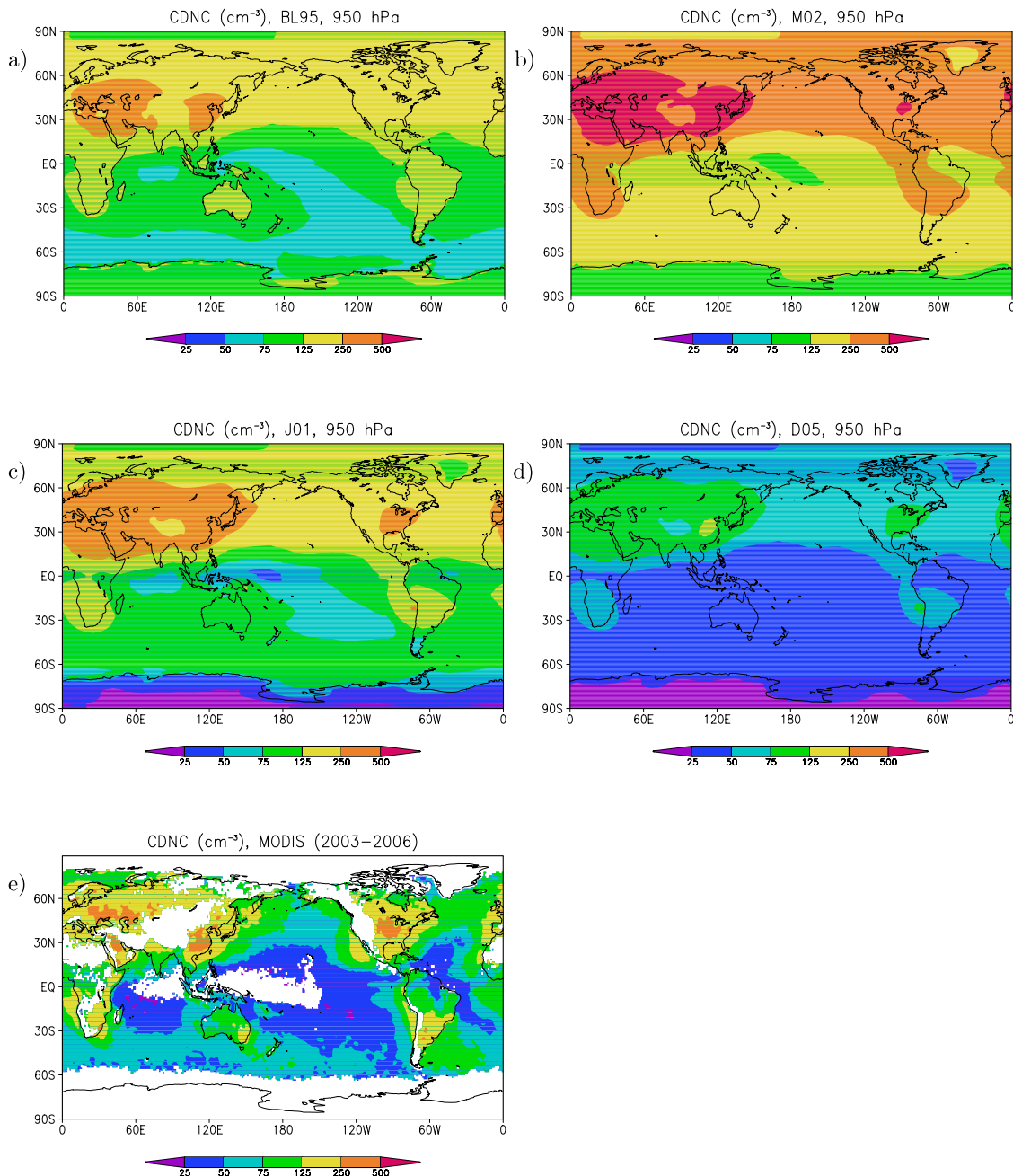


Figure 2. Cloud Droplet Number Concentration (CDNC) (cm^{-3}) at 950 hPa as predicted following the method of (a) BL95, (b) J01, (c) M02 and (d) D05 and (e) boundary layer CDNC as observed by MODIS.

tions and the other with aerosol concentrations corresponding to present day (PD) conditions. Anthropogenic changes in model parameters were thereafter calculated as the difference between the two simulations (subtracting PI values from PD values). We do not include the direct, semi-direct and second indirect aerosol effects in our simulations. Each simulation was carried out for 5 years, using climatological sea surface temperatures and sea ice extent. For all simulations, the CDNC is restricted to values higher than 5 cm^{-3} .

3. Results and Discussion

[16] As evident from Figures 2a–2d, the four different CDNC schemes lead to significant differences in the CDNC

values at 950 hPa (shown here for PD simulations). The highest CDNCs are produced by M02, while the D05 CDNC parameterization resulted in the lowest CDNCs. Similarly, as seen from Table 1, the anthropogenic changes in CDNC values at 950 hPa differ by one order of magnitude, leading to anthropogenic changes in the net radiative flux at the top of the atmosphere ranging from -0.62 W/m^2 to -1.94 W/m^2 . This range is dominated by the anthropogenic change in shortwave radiation, as the change in longwave radiation is always positive and never exceeds 0.12 W/m^2 in any of the simulations. Generally, large anthropogenic changes in CDNC are expected to yield large AIEs. This is also confirmed by Table 1. However, the AIE is not only dependent on the anthropogenic CDNC

Table 1. Aerosol Indirect Effect and Corresponding Anthropogenic Changes in CDNC at 950 hPa for the Four CDNC Schemes

CDNC Scheme	Aerosol		Δ CDNC at 950 hPa (cm^{-3})
	Indirect Effect (W/m^2)	Unperturbed CDNC at 950 hPa (cm^{-3})	
BL95	-0.91	111.4	22.0
J01	-0.97	107.8	39.8
M02	-1.94	158.7	123.1
D05	-0.62	41.9	10.5

perturbation, but also on the optical thickness of the unperturbed clouds. Typically, clouds with relatively low CDNCs are more susceptible to a CDNC perturbation than clouds with high CDNCs [e.g., *Koren et al.*, 2008]. Consequently, the modest anthropogenic CDNC perturbation by D05 still leads to a significant AIE response of -0.62 W/m^2 , because the unperturbed clouds contain few cloud droplets in this case. Similarly, the high natural CDNC values of M02 correspond to a model state which is relatively insensitive to additional cloud droplets. Hence, a CDNC increase ten times larger than by D05 leads to an AIE of -1.94 W/m^2 , i.e., only about three times larger than the AIE by D05. Despite this CDNC saturation effect, the spread in AIE arising from varying the CDNC prediction is significant.

[17] Figure 2e shows boundary layer CDNC derived from four years (2003–2006) of Moderate Resolution Imaging Spectroradiometer (MODIS) data using the methodology described by *Bennartz* [2007]. This study utilizes Level-3 daily atmospheric product, termed Atmospheric Daily Global Joint Product (Collection 5) available at the NASA Goddard Earth Sciences (GES) Distributed Active Archive Center (DAAC). The data is available on a 1×1 degree grid. In addition to the ocean-only data reported by *Bennartz* [2007] we also present CDNC data over land in this study. This data is derived using the same methodology applied to MODIS cloud optical parameters over land. The accuracy of CDNC retrievals over water surfaces is discussed in detail by *Bennartz* [2007]. Over land surfaces the accuracy of the product might be further reduced by unresolved variations in surface albedo. The averaging period of 4 years ensures that random variations are sufficiently reduced to ensure a high accuracy of the average CDNC. However, in particular over land, the effects of undetected elevated aerosol layers above clouds might potentially lead to a systematic underestimation of retrieved CDNC, as discussed by *Bennartz and Harshvardhan* [2007]. For reasonably thin undetected aerosol layers, this effect will be about 20% at most and will thus be much smaller than the differences between the different CDNC schemes.

[18] As evident from Figure 2, M02 significantly overestimates CDNC compared to the MODIS data, while D05 underestimates CDNC, particularly over land. J01 and BL95 both compare favourably to the MODIS data, although J01 seems to predict too high CDNCs over the ocean. This overestimation is more pronounced at mid-latitudes, indicating that droplets formed on sea salt generated by high wind speeds may be causing this overestimation. It is interesting to note that BL95, representing the oldest and simplest CDNC scheme considered in this study, leads to the best comparison with observations. Comparing simulated CDNC at 850 hPa rather than 950 hPa will not significantly affect the above conclusions. However, the comparison is likely to be sensi-

tive to the present-day aerosol fields, and simulations with aerosol fields deviating significantly from the ones employed here could lead to different conclusions. As the IFS has traditionally been employed in forecast rather than climate mode, it is reassuring that global cloud properties (liquid water path, ice water path and cloud cover) compare well with observed values (Table 2). Additionally, there is little variation in these variables for the different simulations. As aerosols effects on the hydrological cycle are not explicitly taken into account in this study, this is to be expected.

4. Conclusion

[19] In this study, we have demonstrated that the various CDNC schemes applied in the coupled model simulations presented in the IPCC AR4 yield a first aerosol indirect effect ranging from -0.62 W/m^2 to -1.94 W/m^2 , in simulations where aerosol fields and all other aspects of the model remained unchanged. This result indicates that most of the spread in the anthropogenic shortwave forcings from coupled simulations in the IPCC AR4 could possibly be explained simply by the different empirical relationships between aerosol mass and cloud droplet number concentration used in these models. However, there are also uncertainties associated with shortwave forcings arising from other processes, for instance the direct aerosol effect or land use changes. Additionally, the aerosol indirect effect is strongly dependent on model state (e.g., amount of low vs. high clouds) and pre-industrial vs. present-day aerosol fields. Hence, the same study carried out in a different model and/or with different aerosol fields could yield different results. Nevertheless, the spread in AIEs obtained in this study is significant, suggesting that the AIE is the primary contributor to the spread in estimates of anthropogenic shortwave forcings. Based on radiative transfer calculations for an idealized cloud case (i.e., fixed surface albedo, latitude, cloud cover, etc.), *McComiskey and Feingold* [2008] found a set of different empirical relationships between CDNC and aerosol concentrations to yield a wide range of aerosol indirect forcings. Here, we have qualitatively confirmed their results in a non-idealized global context. Despite the wide uncertainty in AIE associated with empirical relationships, they are likely to be employed in global climate model (GCM) simulations for years to come, as they are relatively easy to implement in models and computationally inexpensive. The latter makes them particularly attractive for transient climate simulations. Hence, the AIE uncertainty range reported in this study should be kept in mind when comparing transient climate simulations in the future.

Table 2. Observed and Modeled Global Average Cloud Cover, Ice Water Path and Liquid Water Path^a

	Cloud Cover (%)	Ice Water Path (g/m^2)	Liquid Water Path (g/m^2)
EC-Earth	62.0–62.2	28.7–29.0	58.4–59.9
Observations	62–67	29.4	50–84

^aTotal cloud cover observations are obtained from surface observations [*Hahn et al.*, 1994], the International Satellite Cloud Climatology Project (ISCCP) [*Rossow and Schiffer*, 1999] and MODIS data [*King et al.*, 2003]. The LWP observations are from SSM/I [*Weng and Grody*, 1994; *Greenwald et al.*, 1993; *O'Dell et al.*, 2008], and IWP is derived from ISCCP data [*Storelvmo et al.*, 2008].

[20] **Acknowledgments.** We thank the European Centre for Medium-Range Weather Forecasts (ECMWF) for providing computing time within the special project SPCHCLAI and gratefully appreciate the user support for the help with the supercomputing facility. We are also thankful to the Swiss Federal Office of Meteorology and Climatology (MeteoSwiss) for supporting this study with additional computing time. Finally, we would like to thank two anonymous reviewers for comments that led to improvements of the paper.

References

- Baker, M. B., and T. Peter (2008), Small-scale cloud processes and climate, *Nature*, *451*, 299–300.
- Bennartz, R. (2007), Global assessment of marine boundary layer cloud droplet number concentration from satellite, *J. Geophys. Res.*, *112*, D02201, doi:10.1029/2006JD007547.
- Bennartz, R., and Harshvardhan (2007), Correction to “Global assessment of marine boundary layer cloud droplet number concentration from satellite”, *J. Geophys. Res.*, *112*, D16302, doi:10.1029/2007JD008841.
- Boucher, O., and U. Lohmann (1995), The sulfate-CCN-cloud albedo effect: A sensitivity study with two general circulation models, *Tellus, Ser. B*, *47*, 281–300.
- Chen, Y., and J. Penner (2005), Uncertainty analysis for estimates of the first indirect effect, *Atmos. Chem. Phys.*, *5*, 2935–2948.
- Dufresne, J. L., J. Quaas, O. Boucher, S. Denvil, and L. Fairhead (2005), Contrasts in the effects on climate of anthropogenic sulfate aerosols between the 20th and the 21st century, *Geophys. Res. Lett.*, *32*, L21703, doi:10.1029/2005GL023619.
- Forster, P., et al. (2007), Changes in atmospheric constituents and in radiative forcing, in *Climate Change 2007: The Physical Science Basis. Contribution of Working Group I to the Fourth Assessment Report of the Intergovernmental Panel on Climate Change*, edited by S. Solomon et al., chap. 2, pp. 129–234, Cambridge Univ. Press, Cambridge, U. K.
- Fouquart, Y. (1987), Radiative transfer in climate modeling, in *Physically-Based Modeling and Simulation of Climate and Climate Changes*, edited by M. E. Schlesinger, pp. 223–283, Kluwer Acad., Dordrecht, Netherlands.
- Greenwald, T. J., G. L. Stevens, T. H. V. Har, and D. L. Jackson (1993), A physical retrieval of cloud liquid water over the global oceans using special sensor microwave/imager (SSM/I) observations, *J. Geophys. Res.*, *98*, 18,471–18,488.
- Hahn, C. J., S. G. Warren, and J. London (1994), Climatological data for clouds over the globe from surface observations 1982–1991: The total cloud edition, *Tech. Rep., ORNL/CDIAC-72 NDP-026A*, Oak Ridge Natl. Lab., Oak Ridge, Tenn.
- Jones, A., D. L. Roberts, and A. Slingo (1994), A climate model study of indirect radiative forcing by anthropogenic sulphate aerosols, *Nature*, *370*, 450–453.
- Jones, A., D. L. Roberts, M. J. Woodage, and C. E. Johnson (2001), Indirect sulphate aerosol forcing in a climate model with an interactive sulphur cycle, *J. Geophys. Res.*, *106*, 20,293–20,310.
- King, M. D., W. P. Menzel, Y. J. Kaufmann, D. Tanre, B. C. Gao, S. Platnick, S. A. Ackerman, L. Remer, R. Pincus, and P. A. Hubanks (2003), Cloud and aerosol properties, precipitable water, and profiles of temperature and water vapor from MODIS, *IEEE Trans. Geosci. Remote Sens.*, *41*, 442–458.
- Koren, I., J. W. Martins, L. A. Remer, and A. Afargan (2008), Smoke invigoration versus inhibition of clouds over the Amazon, *Science*, *321*, 946–949.
- Martin, G. M., D. W. Johnson, and A. Spice (1994), The measurement and parameterization of effective radius of droplets in warm stratocumulus clouds, *J. Atmos. Sci.*, *51*, 1823–1842.
- McComiskey, A., and G. Feingold (2008), Quantifying error in the radiative forcing of the first aerosol indirect effect, *Geophys. Res. Lett.*, *35*, L02810, doi:10.1029/2007GL032667.
- Meehl, G., et al. (2007), Global climate projections, in *Climate Change 2007: The Physical Science Basis. Contribution of Working Group I to the Fourth Assessment Report of the Intergovernmental Panel on Climate Change*, edited by S. Solomon et al., chap. 10, pp. 747–845, SM10-1–SM10-8, Cambridge Univ. Press, Cambridge, U. K.
- Menon, S., A. D. D. Genio, D. Koch, and G. Tselioudis (2002), GCM simulations of the aerosol indirect effect: Sensitivity to cloud parameterization and aerosol burden, *J. Atmos. Sci.*, *59*, 692–713.
- O’Dell, C. W., F. J. Wentz, and R. Bennartz (2008), Cloud liquid water path from satellite-based passive microwave observations: A new climatology over the global oceans, *J. Clim.*, *21*, 1721–1739.
- O’Dowd, C. D., M. H. Smith, I. E. Consterdine, and J. A. Lowe (1997), Marine aerosol, sea salt, and the marine sulphur cycle: A short review, *Atmos. Environ.*, *31*, 73–80.
- O’Dowd, C. D., J. A. Lowe, and M. H. Smith (1999), Coupling sea-salt and sulphate interactions and its impact on cloud droplet concentration predictions, *Geophys. Res. Lett.*, *26*, 1311–1314.
- Penner, J. E., J. Quaas, T. Storelvmo, T. Takemura, O. Boucher, H. Guo, A. Kirkevåg, J. Kristjansson, and O. Seland (2006), Model intercomparison of indirect aerosol effects, *Atmos. Chem. Phys.*, *6*, 3391–3405.
- Rossow, W. B., and R. A. Schiffer (1999), Advances in understanding clouds from ISCCP, *Bull. Am. Meteorol. Soc.*, *80*, 2261–2287.
- Storelvmo, T., J. E. Kristjansson, and U. Lohmann (2008), Aerosol influence on mixed-phase clouds in CAM-Oslo, *J. Atmos. Sci.*, *60*, 3214–3230.
- Tiedke, M. (1993), Representation of clouds in large-scale models, *Mon. Weather Rev.*, *121*, 3040–3061.
- Twomey, S. (1974), Pollution and the planetary albedo, *Atmos. Environ.*, *8*, 1251–1256.
- Weng, F., and N. C. Grody (1994), Retrieval of cloud liquid water using the Special Sensor Microwave Imager (SSM/I), *J. Geophys. Res.*, *99*, 25,535–25,551.

R. Bennartz, Department of Atmospheric and Oceanic Sciences, University of Wisconsin-Madison, Madison, WI 53706, USA.

U. Lohmann and T. Storelvmo, Institute for Atmospheric and Climate Sciences, ETH-Zurich, Universitaetsstrasse 16, CH-8092 Zurich, Switzerland. (trude.storelvmo@env.ethz.ch)